







## Biodegradation of low-density polyethylene films commercially labeled as biodegradable pretreated with UV-B radiation by *Pleurotus ostreatus* grown in liquid fermentation

## Biodegradación de películas de polietileno de baja densidad comercialmente etiquetadas como biodegradables pretratadas con radiación UV-B por *Pleurotus ostreatus* crecido en fermentación líquida

Ariadna Denisse Andrade-Alvarado<sup>1</sup>, Rosario González-Mota<sup>1\*</sup>, Angel González-Márquez<sup>2</sup>, Carmen Sánchez<sup>2\*</sup>

<sup>1</sup> Optoelectronics Laboratory, Tecnológico Nacional de México, Instituto Tecnológico de Aguascalientes, Aguascalientes, Mexico.

<sup>2</sup> Research Centre for Biological Sciences, Universidad Autónoma de Tlaxcala, Tlaxcala, Mexico.

Corresponding authors

E-mail addresses: [rosario.gm@aguascalientes.tecnm.mx](mailto:rosario.gm@aguascalientes.tecnm.mx) (R. González-Mota); [carmen.sanchezh@uatx.mx](mailto:carmen.sanchezh@uatx.mx) (C. Sánchez)

Article history:

Received: 15 August 2024 / Received in revised form: 17 November 2024 / Accepted: 1 December 2024 / Published online: 19 December 2024.

<https://doi.org/10.29267/mxjb.2024.9.4.52>

### ABSTRACT

Biodegradable plastics are eco-friendly materials that can be safely incorporated into the environment to reduce plastic pollution. In this work, *Pleurotus ostreatus* was grown in unirradiated (UnBPE) and UV-B irradiated low-density polyethylene films (IrBPE) commercially labeled as biodegradable for four weeks in liquid fermentation. Fungal growth, laccase (Lac), lignin peroxidase (LiP), unspecific peroxygenase (UnP), and manganese peroxidase (MnP) activities, and contact angle, as well as changes in the surface morphology and chemical structure of the samples using SEM and FTIR spectroscopy, respectively, were evaluated. Production of fungal biomass was similar in both IrBPE and UnBPE samples. *P. ostreatus* showed higher enzyme activities in IrBPE than in UnBPE.

From all the enzymes tested, Lac had the highest activity (5836.69 U/L) followed by LiP (2789.15 U/L), UnP (2681.04 U/L), and MnP (983.37 U/L) in IrBPE. The lowest contact angle was observed at week four, decreasing from 67.33° to 50.66° for IrBPE. The FTIR surface spectra of the samples showed an increase in distinctive oxidation bands in the polymer chain, corresponding to functional groups such as carbonyls, vinyls, and hydroxyls. IrBPE showed fractures on its surface. Low-density polyethylene commercially labeled as biodegradable enhanced its biodegradation when exposed to pretreatment with UV-B radiation.

**Keywords:** Biodegradation, enzyme, FTIR spectroscopy, photodegradation, *Pleurotus ostreatus*, polyethylene.

## RESUMEN

Los plásticos biodegradables son materiales ecológicos que se pueden incorporar de forma segura al medio ambiente para reducir la contaminación por estos materiales. En este trabajo, *Pleurotus ostreatus* se creció sobre películas de polietileno de baja densidad etiquetadas comercialmente como biodegradables no irradiadas (UnBPE) e irradiadas con UV-B (IrBPE) durante cuatro semanas en fermentación líquida. Se evaluó el crecimiento de hongos; las actividades de lacasa (Lac), lignin peroxidasa (LiP), peroxigenasa inespecífica (UnP) y manganeso peroxidasa (MnP), y el ángulo de contacto, así como los cambios en la morfología de la superficie y en la estructura química de las películas de BPE mediante SEM y espectroscopia FTIR, respectivamente. La producción de biomasa fúngica fue similar en las películas de IrBPE y UnBPE. *P. ostreatus* presentó mayor actividad enzimática en IrBPE que en UnBPE. De todas las enzimas analizadas, Lac presentó la actividad más alta (5836.69 U/L), seguida de LiP (2789.15 U/L), UnP (2681.04 U/L) y MnP (983.37 U/L) en IrBPE. El menor ángulo de contacto se presentó en la cuarta semana, disminuyendo de 67.33° a 50.66° para el IrBPE. El espectro de infrarrojo de la superficie de las muestras mostró un aumento en las bandas de oxidación distintivas en la cadena de polímero, correspondientes a grupos funcionales como carbonilos, vinilos e hidroxilos. IrBPE presentó fracturas en su superficie. Estos resultados muestran que el polietileno de baja densidad etiquetado comercialmente como biodegradable mejoró su biodegradación cuando se expuso al pretratamiento con radiación UV-B.

**Palabras clave:** Biodegradación, enzima, espectroscopía infrarroja, fotodegradación, *Pleurotus ostreatus*, polietileno.

## 1. INTRODUCTION

Plastic polymeric materials are raising concerns due to their increasing production and lack of effective disposal. The release of these polymers into the environment causes contamination with an impact on ecosystems and animal and human health (Yuan *et al.*, 2022). Global plastic production has steadily increased since its introduction in the 1950s, reaching approximately 400 million tons annually. Furthermore, it is estimated that global plastic production will reach 1124 million tons by 2050 (Eriksen *et al.*, 2019), reflecting the

durability and versatility of this material in various applications (Chamas *et al.*, 2020; Lear *et al.*, 2021; Okoffo *et al.*, 2021). This overproduction is due to the fact that most plastic products are single-use items with a short lifespan and take decades or centuries to degrade naturally (Chamas *et al.*, 2020; Ghosh and Jones, 2021).

Specifically, polyethylene (PE) is a polymer of great global importance with various industrial and domestic applications due to its durability, toughness, and low cost (Skariyachan *et al.*, 2022; Zhang *et al.*, 2022; Burelo *et al.*, 2023; Tiago *et al.*, 2023). PE can be classified based on its density into low-density polyethylene (LDPE), medium-density polyethylene, and high-density polyethylene (HDPE), with LDPE and HDPE being the most used (Zhang *et al.*, 2022; He *et al.*, 2024). LDPE represents approximately 20% of commercial plastic waste frequently generated (Fotopoulou and Karapanagioti, 2017; Dimassi *et al.*, 2024).

PE is a high molecular weight polymer consisting mainly of linear carbon and hydrogen chains bonded by single bonds. PE has low degradability under environmental conditions due to the lack of reactive and hydrolyzable groups (Restrepo-Flórez *et al.*, 2014; Zhang *et al.*, 2022). Effective degradation of PE requires the polymer chain oxidation and reduces its molecular weight (Han *et al.*, 2024).

Conventional PE can take years to degrade in the environment. Therefore, to mitigate plastic pollution, biodegradable plastics (BPE) have been developed (Flury and Narayan, 2021; Ghosh and Jones, 2021). BPE contains additives, plasticizers, and pigments that accelerate its degradation through microorganism action, mineralizing into H<sub>2</sub>O, CO<sub>2</sub>, CH<sub>4</sub>, and microbial biomass (Flury and Narayan, 2021; Sánchez, 2021; Zhou *et al.*, 2023; Kaing *et al.*, 2024; Zhang *et al.*, 2024). BPE use is expected to increase to 5.3 million tons by 2026 (Moshood *et al.*, 2021; Zhang *et al.*, 2024).

Some types of fungi degrade PE due to their mycelial growth, which penetrates the polymer surface and initiates biodegradation. Moreover, fungi can survive under stressful conditions by secreting extracellular enzymes to fragment the polymeric chains, and then use their intracellular enzymes to assimilate the monomers to finally mineralize the polymer (Sánchez, 2020; Ali *et al.*, 2021). However, due to the PE chemical composition, an abiotic oxidation process is necessary prior to biodegradation to reduce molecular weight. These changes could be achieved through photooxidation, thermodegradation or chemical hydrolysis (Flury and Narayan, 2021; Ghosh and Jones, 2021; Taghavi *et al.*, 2021; Patel *et al.*, 2022; Han *et al.*, 2024). In this context, UV-B radiation photooxidation causes polymer chain scission and functional groups formation like hydroxyls and carbonyls, changing the PE surface hydrophilicity and promoting microorganism attachment to the PE surface (Chamas *et al.*, 2020; Zhang *et al.*, 2020; Zhang *et al.*, 2024). Currently, studies on BPE photooxidation are limited (Kaing *et al.*, 2024).

During PE biodegradation, oxidoreductase enzymes are secreted by hyphae to fragment the PE polymer chain and generate low molecular weight chains that can be assimilated and mineralized by fungal cells (Okal *et al.*, 2023; He *et al.*, 2024). Microorganisms used to degrade PE include *Fusarium* sp., *Aspegillus* sp., *Penicillium* spp., *Helminthosporium* sp., *Spicaria* spp., *Agrocybe aegerita*, *Ganoderma lucidum*, *Pleurotus ostreatus*, *Trametes versicolor*, *Alternaria solani*, and *Geomyces pannorum* (Volke-Sepúlveda *et al.*, 2002; Kyaw *et al.*, 2012; Kumar and Chandra, 2020; Amobonye *et al.*, 2021; Spina *et al.*, 2021; Bertolacci *et al.*, 2022; Okal *et al.*, 2023). Specifically, the fungus *P. ostreatus* produce laccase (Lac), manganese peroxidase (MnP), lignin peroxidase (LiP), and unspecific peroxygenase (UnP), capable of degrading lignocellulosic residues (Chang and Chang, 2016; Kumar and Chandra, 2020; Bertolacci *et al.*, 2022; Okal *et al.*, 2023).

In this study, *P. ostreatus* was grown in unirradiated (UnBPE) and UV-B irradiated low-density polyethylene films (IrBPE) commercially labeled as biodegradable for four weeks in liquid fermentation. Fungal growth, Lac, LiP, UnP, and MnP activities, contact angle, and changes in the surface morphology and chemical structure of the samples using SEM and FTIR spectroscopy were evaluated.

## **2. MATERIALS AND METHODS**

### **2.1. Strain**

The fungal strain *P. ostreatus* Po7-CICBUAT was obtained from the culture collection of the Research Centre for Biological Sciences at the Universidad Autónoma de Tlaxcala (CICB, Tlaxcala, Mexico). The strain was grown on malt extract agar and incubated at  $27 \pm 1$  °C for 5 d, then stored at 2 °C until used as inoculum.

### **2.2. Polyethylene samples preparation**

BPE films were taken from a commercial bag labeled as biodegradable. The irradiation time was determined based on a preliminary study described by González-Márquez *et al.*, (2024). BPE films, size of 10 cm x 10 cm, were homogeneously irradiated with  $3.5 \times 10^{-4}$  W/cm<sup>2</sup> of UV-B radiation (280-320 nm) for 20 d using a BYTEK UV-B chamber (model Ultraviolet Multiprom Eraser, China). The IrBPE and UnBPE films (2.5 cm x 2.5 cm) were washed with a sterile liquid soap solution (50 mL of commercial liquid soap and 50 mL of distilled water). For storage, the BPE films were placed in 70% ethanol in a sterile environment. The BPE films were used once the alcohol evaporated.

### **2.3. Media and culture conditions**

The culture medium was prepared using wheat straw extract as a base component. 100 g of wheat straw were boiled for 30 minutes, filtered to remove solid residues, and adjusted to 1 L with distilled water. The following nutrients (g/L) were added to the base medium: 25.0 malt extract, 5.0 yeast extract, 0.1872 K<sub>2</sub>HPO<sub>4</sub>, 0.2032 MgNO<sub>3</sub>, 0.5 Ca(H<sub>2</sub>PO<sub>4</sub>)<sub>2</sub>, 1.0 MgSO<sub>4</sub>, 0.005 FeSO<sub>4</sub>, 0.007 ZnSO<sub>4</sub>, 0.009 MnSO<sub>4</sub>, and 0.011 CuSO<sub>4</sub>. A BPE film (either IrBPE or UnBPE) was placed in a 125 mL Erlenmeyer flask with 50 mL of culture medium. Each flask was inoculated with 10 fragments of mycelium (8 mm in diameter), taken from the periphery of a colony grown on malt extract agar. Cultures were incubated at 27 °C in a rotary shaker (Prendo INO 650V-7, Mexico) at 120 rpm for 4 weeks. Samples were taken weekly in triplicate.

### **2.4. Biomass production and enzyme activity assay**

The cultures were vacuum filtered using pre-dried filter paper (Whatman No. 4) at 60 °C for 48 h with a vacuum pump (Millipore, Merck, Germany). Biomass production (X) was quantified by dry weight difference (g/L) between the filter paper and the filter paper with dried biomass at 60 °C for 48 h (Ríos-González *et al.*, 2019).

The supernatant was used to determine enzyme activity using a UV-VIS spectrophotometer Jenway, model Basic 7305 (Stone, Staffs, UK). One unit of enzyme activity (U) is defined

as the amount of enzyme required to transform 1  $\mu\text{mol}$  of substrate per minute. The calculated enzymatic parameters included enzymatic yield ( $Y_{E/X}$ ) based on the ratio of maximum enzyme production ( $E_{\text{max}}$ ) (U/L) and maximum biomass production ( $X_{\text{max}}$ ) (g/L); and enzymatic productivity ( $P_{\text{RO}}$ ) with the ratio of  $E_{\text{max}}$  (U/L) to the fermentation time for  $E_{\text{max}}$  (Bettin *et al.*, 2011).

The reaction mixture to determine Lac activity contained 900  $\mu\text{L}$  of dimethoxyphenol (DMP) as substrate in 0.1 M sodium acetate buffer solution at pH 4.5 and 100  $\mu\text{L}$  of supernatant, incubated at 40 °C for 1 min. DMP oxidation was measured by UV-Vis spectrophotometry at a wavelength ( $\lambda$ ) at 468 nm for 1 minute ( $\epsilon_{469} = 49600 \text{ 1/M cm}$ ) (Camacho-Morales *et al.*, 2017; González-Márquez and Sánchez, 2024). The reaction mixture for determining MnP activity consisted of adding 75  $\mu\text{L}$  of 1 mM manganese sulfate tetrahydrate ( $\text{MnSO}_4$ ), 790  $\mu\text{L}$  of 0.1 M sodium tartrate buffer solution at pH 4.2, 50  $\mu\text{L}$  of 40 mM  $\text{H}_2\text{O}_2$ , 75  $\mu\text{L}$  of 10 mM guaiacol, and 10  $\mu\text{L}$  of supernatant, which was incubated at 25°C for 5 min using 10 mM guaiacol as a substrate. The oxidation was monitored by UV-Vis spectrophotometry, measuring absorbance at  $\lambda$  of 334 nm for 1 min ( $\epsilon_{334} = 18300 \text{ 1/M cm}$ ) (Camacho-Morales *et al.*, 2017; González-Márquez *et al.*, 2024). UnP activity was evaluated at 25 °C by incubating the reaction mixture for 5 min using 40 mM veratryl alcohol as the substrate. The reaction mixture consisted of 100  $\mu\text{L}$  of 40 mM veratryl alcohol, 840  $\mu\text{L}$  of 0.1 M sodium citrate buffer at pH 4.5, 50  $\mu\text{L}$  of 40 mM  $\text{H}_2\text{O}_2$ , and 10  $\mu\text{L}$  of supernatant. The oxidation of veratryl alcohol was measured by UV-Vis spectrophotometry at  $\lambda$  of 310 nm ( $\epsilon_{310} = 9300 \text{ 1/M cm}$ ) for 1 min (González-Rodríguez *et al.*, 2023; González-Márquez *et al.*, 2024). LiP activity was evaluated at 25 °C by incubating the reaction mixture for 5 min using 40 mM veratryl alcohol as a substrate. The reaction mixture consisted of 200  $\mu\text{L}$  of 40 mM veratryl alcohol, 580  $\mu\text{L}$  of 0.1 M tartrate buffer at pH 4.2, 200  $\mu\text{L}$  of 40 mM  $\text{H}_2\text{O}_2$ , and 20  $\mu\text{L}$  of supernatant. The oxidation of veratryl alcohol was measured by UV-Vis spectrophotometry at  $\lambda$  of 310 nm ( $\epsilon_{310} = 9300 \text{ 1/M cm}$ ) for 1 min (Arora and Gill, 2001; Ocaña-Romo *et al.*, 2024; González-Márquez *et al.*, 2024).

## 2.5. FTIR analysis of polyethylene samples

Changes in the chemical structure of BPE were analyzed using the Thermo Nicolet iS10 infrared spectrometer (Massachusetts, USA) with a Ge mirror provided by the Instrumental Analysis Laboratory at the Tecnológico Nacional de México (Instituto Tecnológico de Aguascalientes), employing the attenuated total reflectance (ATR) technique. The absorption spectra of the BPE films were scanned 64 times to give a final optimized spectra with a resolution of 4  $\text{cm}^{-1}$  in the range of 4000-500  $\text{cm}^{-1}$ .

The infrared spectra were processed using Origin Pro-2023 software, normalizing the absorbance to its maximum value. The hydroxyl index (HI) of the BPE film was calculated using the ratio of the intensity of the hydroxyl group (OH) vibration band at 3400  $\text{cm}^{-1}$  to a constant intensity band (719  $\text{cm}^{-1}$ ) (Martínez-Romo *et al.*, 2018). The carbonyl index (CI) of the BPE film was calculated using the ratio of the intensity of the carbonyl group (C=O) vibration band at 1652  $\text{cm}^{-1}$  to a constant intensity band (719  $\text{cm}^{-1}$ ) (Gómez-Méndez *et al.*, 2018; Prata *et al.*, 2020). The vinyl index (VI) of the BPE film was determined using the ratio of the intensity of the out-of-plane  $\text{CH}_2$  deformation vibration band of the vinylidene group at 875  $\text{cm}^{-1}$  to a constant intensity band (719  $\text{cm}^{-1}$ ) (Gómez-Méndez *et al.*, 2018; Prata *et al.*, 2020).

## 2.6. Surface hydrophobicity analysis of polyethylene samples after fungal growth

The surface hydrophobicity of the samples was calculated by measuring the contact angle, placing 5  $\mu$ L of distilled water on the sample to form a droplet (Lamour *et al.*, 2010). Images to assess the contact angle were captured using the iPhone 13 Pro camera (ISO 250, f 1.8, 1/60 s) and processing was performed using ImageJ software (version 1.53).

## 2.7. Detection of surface change in polyethylene samples using scanning electron microscopy

Morphological changes in BPE were analyzed using a scanning electron microscope (SEM). SEM analysis was conducted using energy-dispersive X-ray spectroscopy (EDX) for elemental composition analysis with a Hitachi SU3500 equipment, operating at a voltage of 5 kV, an analysis surface of 17 mm, and a magnification of 1000x.

## 2.8. Statistical analysis

The results obtained were verified under the assumptions of normality (Shapiro-Wilk Test) and homoscedasticity (Levene's Test). Analysis of variance (ANOVA) was performed for the statistical evaluations followed by the post-hoc Tukey test. All calculations were performed with statistical analysis system (SAS, free software trials) program, with a significance level of  $p < 0.05$ . Data are reported as the mean  $\pm$  standard deviation of experiments performed in triplicate.

# 3. RESULTS

## 3.1. Biomass production and enzyme activity assay

Biomass production during the biodegradation process of BPE by *P. ostreatus* is shown in Fig. 1. The maximum biomass production ( $X_{max}$ ) was achieved at week 3 of biodegradation with 12.35 g/L and 12.85 g/L for IrBPE and UnBPE, respectively. *P. ostreatus* exhibited an exponential growth from week 0 to week 1, and a stationary phase from week 1 to week 3 in both samples.

*P. ostreatus* secreted Lac, MnP, LiP, and UnP in media supplemented with either IrBPE or UnBPE (Fig. 2). The maximum Lac production was achieved at the first week of fermentation, with 5836.69 U/L and 5527.79 U/L for IrBPE and UnBPE, respectively (Fig. 2a). MnP production was observed at week 2 of fermentation, with a maximum activity of 983.37 U/L for IrBPE and 927.14 U/L for UnBPE (Fig. 2b). *P. ostreatus* secreted UnP from week 2 of fermentation and increased during the fermentation, reaching maximum activity at week 4 (2681.04 U/L for IrBPE and 2329.74 U/L for UnBPE) (Fig. 2c). LiP was produced by *P. ostreatus* at the beginning of fermentation, with maximum activity of 2789.15 U/L for IrBPE and 2562.72 U/L for UnBPE at week 3 of fermentation, whose activity decreased after this time (3 weeks) of fermentation (Fig. 2d).

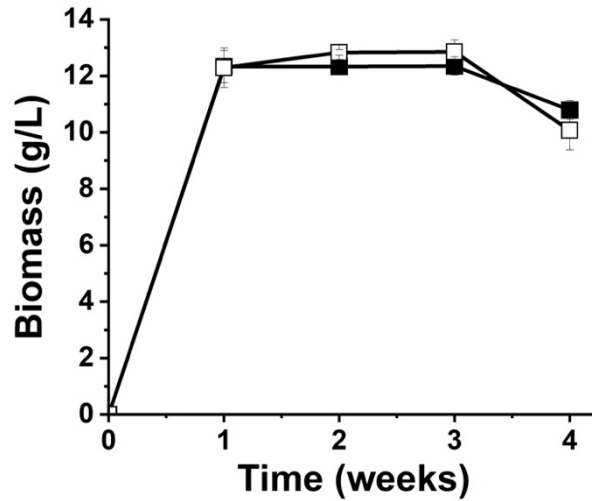


**Fig. 1.** Biomass production by *P. ostreatus* grown on IrBPE (■) and UnBPE (□) in liquid fermentation.

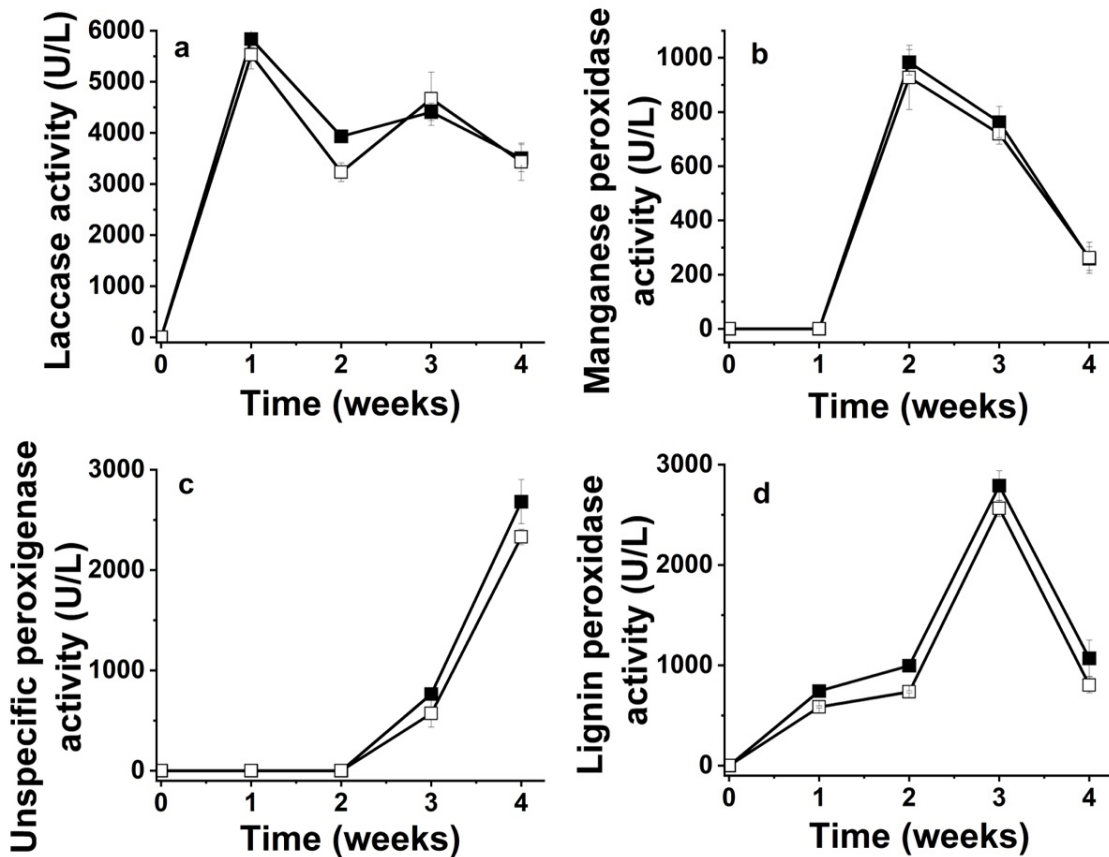


**Fig. 2.** Enzymatic activity of laccase (a), manganese peroxidase (b), unspecific peroxygenase (c), and lignin peroxidase (d) by *P. ostreatus* grown on IrBPE (■) and UnBPE (□) in liquid fermentation.

Table 1 shows the enzymatic parameters for Lac, MnP, UnP, and LiP produced by *P. ostreatus* over 4 weeks in liquid fermentation. The IrBPE films exposed to biodegradation had significantly higher enzyme production, yield, and productivity for the enzymes reported in this study, compared to the UnBPE samples. Furthermore, the Lac enzyme was the one produced in the highest amount by *P. ostreatus* for both films.

**Table 1.** Enzymatic parameters of Lac, MnP, UnP, and LiP produced by *P. ostreatus* grown on IrBPE and UnBPE during 4 weeks of liquid fermentation.

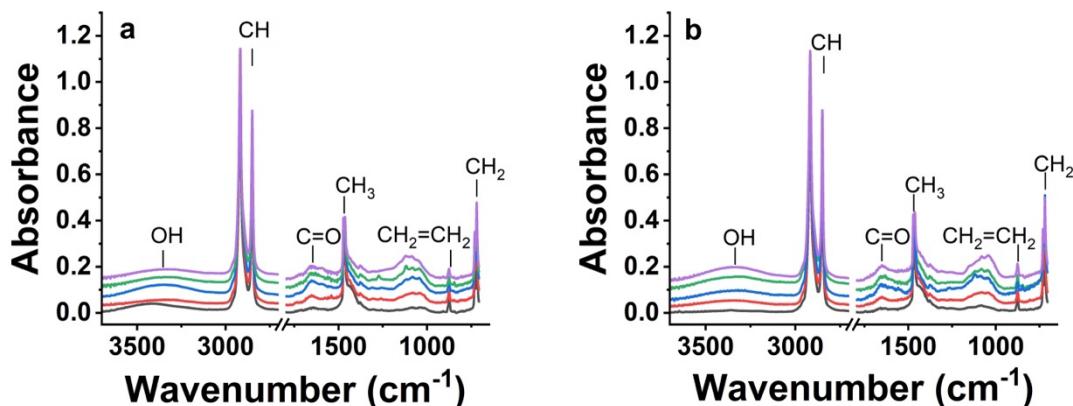
Enzymatic parameters	BPE samples	
	IrBPE	UnBPE
<b>Laccase</b>		
$E_{max}$ (U/L)	5836.69 <sup>a</sup> ± 166.85	5527.79 <sup>b</sup> ± 277.12
$Y_{E/X}$ (U/gX)	472.60 <sup>a</sup> ± 128.94	430.13 <sup>b</sup> ± 15.90
$P_{RO}$ (U/L/h)	34.74 <sup>a</sup> ± 2.34	32.90 <sup>b</sup> ± 1.87
<b>Manganese peroxidase</b>		
$E_{max}$ (U/L)	983.37 <sup>a</sup> ± 45.95	927.14 <sup>b</sup> ± 117.75
$Y_{E/X}$ (U/gX)	79.62 <sup>a</sup> ± 5.43	72.14 <sup>b</sup> ± 7.22
$P_{RO}$ (U/L/h)	2.93 <sup>a</sup> ± 0.58	2.76 <sup>b</sup> ± 0.41
<b>Unspecific peroxygenase</b>		
$E_{max}$ (U/L)	2681.04 <sup>a</sup> ± 219.60	2329.74 <sup>b</sup> ± 252.02
$Y_{E/X}$ (U/gX)	217.09 <sup>a</sup> ± 7.80	181.28 <sup>b</sup> ± 3.93
$P_{RO}$ (U/L/h)	3.99 <sup>a</sup> ± 0.19	2.31 <sup>b</sup> ± 0.98
<b>Lignin peroxidase</b>		
$E_{max}$ (U/L)	2789.15 <sup>a</sup> ± 200.10	2562.72 <sup>b</sup> ± 56.89
$Y_{E/X}$ (U/gX)	225.84 <sup>a</sup> ± 14.00	199.41 <sup>b</sup> ± 3.97
$P_{RO}$ (U/L/h)	5.53 <sup>a</sup> ± 0.40	5.08 <sup>b</sup> ± 0.11

The mean and standard deviation (±) of triplicate experiments are reported. Measurements within the same row with different letters are significantly different. The statistical significance level for the ANOVA is  $p < 0.05$  according to the Tukey test.  $E_{max}$ , maximum enzyme activity;  $P_{RO}$ , enzymatic productivity and  $Y_{E/X}$ , enzymatic yield (see Sect. 2.4).



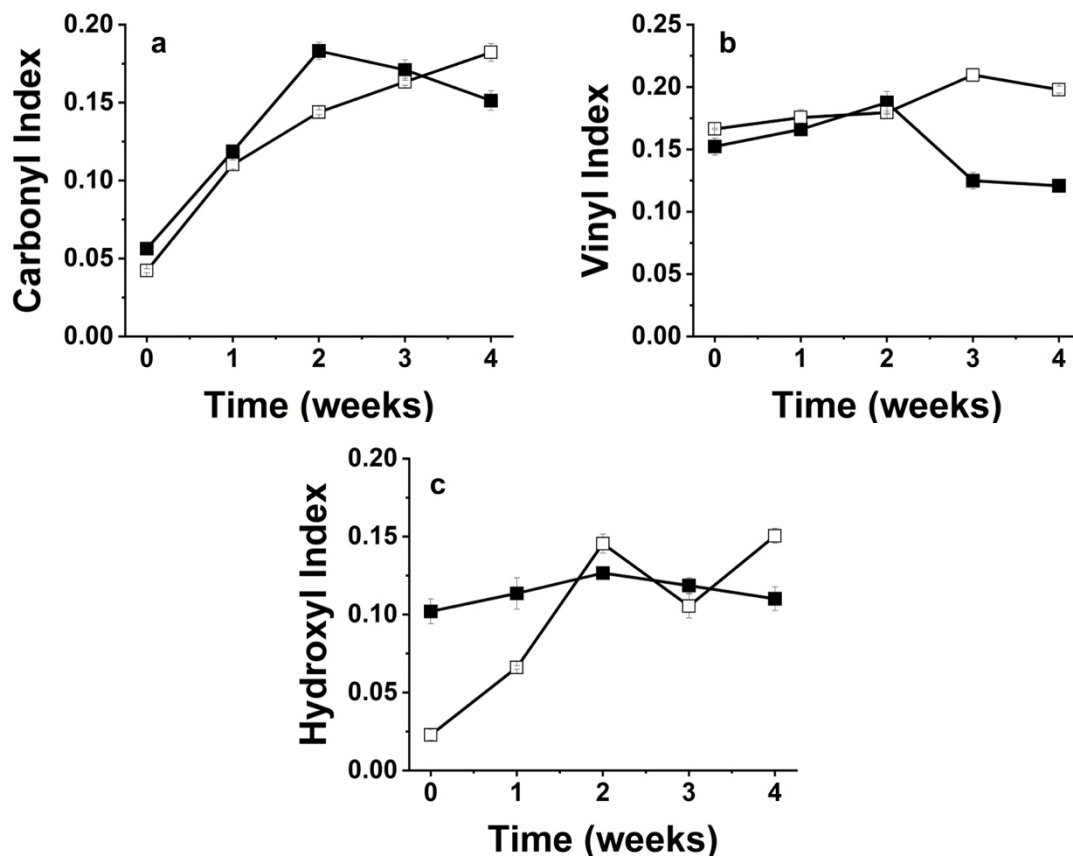
### 3.2. FTIR analysis of polyethylene samples

Fig. 3 shows the FTIR spectra of the surface of IrBPE and UnBPE films from week 0 to week 4 after degradation by *P. ostreatus*. FTIR spectra of the surface of BPE films showed a band in the 3600-3300  $\text{cm}^{-1}$  region, corresponding to hydroxyl (OH) groups. The infrared band corresponding to the carbonyl groups was observed at 1800-1680  $\text{cm}^{-1}$ . The 890  $\text{cm}^{-1}$  band of FTIR spectra of the surface of BPE films corresponding to the out-of-plane deformation vibration of the  $\text{CH}_2$  group in vinylidene.



**Fig. 3.** FTIR spectra of the surface of IrBPE (a) and UnBPE (b) degraded by *P. ostreatus*. Control (black line), week 1 (red line), week 2 (blue line), week 3 (green line), and week 4 (purple line).

BPE films were pre-oxidated with UV-B irradiation, which allows the oxidation of the polymer chain by the action of the fungal enzymes (Fig. 4). UnBPE samples showed higher CI, VI and HI than those CI, VI and HI observed in IrBPE at week 4. The maximum CI, VI, and HI values for the IrBPE samples were 0.18, 0.16, and 0.13, respectively, after two weeks of fermentation, which values decreased during the fermentation. In the case of the UnBPE film, the CI increased throughout the fermentation, while the VI and HI showed an oscillatory pattern.



**Fig. 4.** Carbonyl index (a), vinyl index (b) and hydroxyl index (c) of the surface of IrBPE (■) and UnBPE (□) during 4 weeks of degradation by *P. ostreatus*.

### 3.3. Analysis of surface hydrophobicity of the polyethylene samples after fungal growth

The surface hydrophobicity of BPE samples significantly decreased after degradation by *P. ostreatus* (Table 2). The lowest contact angle was observed at week 4 of liquid fermentation, decreasing from 67.33° to 50.66° for the IrBPE film, and from 78.33° to 60.33° for the UnBPE film. The change in surface hydrophobicity was greater for IrBPE films (3.14 °/Wk) than for UnBPE films (2.6 °/Wk).

### 3.4. Changes in the surface morphology of the polyethylene samples using scanning electron microscopy

Fig. 5 shows the scanning electron micrographs of the surface of IrBPE and UnBPE films after being exposed to degradation by *P. ostreatus*. The additives on the surface of BPE films (irregular particles on the surface) decreased after degradation by *P. ostreatus*. IrBPE showed fractures on its surface, which were due to UV-B irradiation and degradation by *P. ostreatus*. The structural changes on the surface of both films were associated with the

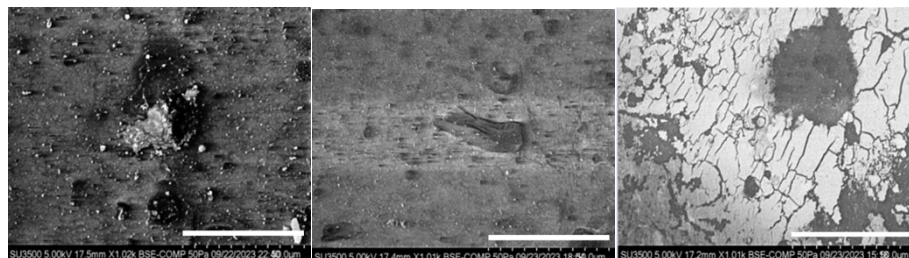
formation of functional groups related to the oxidation of the polymer chain, the reduction of its hydrophobicity, and the enzymatic activity of *P. ostreatus* during fermentation.

**Table 2.** Contact angle (°) of IrBPE and UnBPE films degraded by *P. ostreatus* in liquid fermentation.

Sample	Fermentation time (weeks)				
	0	1	2	3	4
<b>IrBPE</b>	67.33 <sup>a</sup> ± 0.57	63.33 <sup>b</sup> ± 0.57	60.66 <sup>b</sup> ± 0.57	58.00 <sup>c</sup> ± 1.00	50.66 <sup>d</sup> ± 0.57
<b>UnBPE</b>	78.33 <sup>a</sup> ± 1.57	67.33 <sup>b</sup> ± 1.15	63.00 <sup>c</sup> ± 1.00	62.00 <sup>c</sup> ± 1.00	60.33 <sup>d</sup> ± 0.57

The mean and standard deviation (±) of triplicate experiments are reported. Measurements within the same row with different letters are significantly different. The statistical significance level for the ANOVA is  $p < 0.05$  according to the Tukey test.

### IrBPE

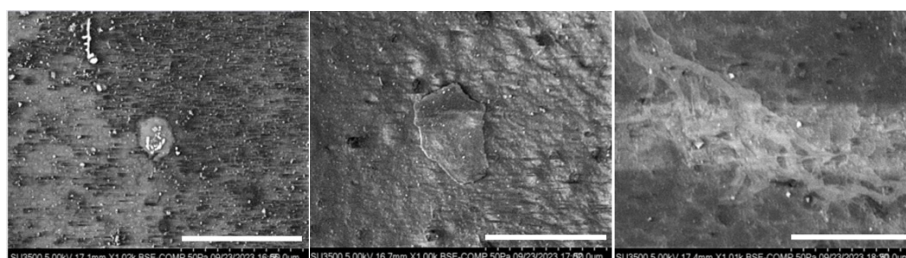


**Control**

**1 Wk**

**3 Wk**

### UnBPE



**Control**

**1 Wk**

**3 Wk**

**Fig. 5.** Scanning electron micrographs of the surface of IrBPE and UnBPE degraded by *P. ostreatus* after 0, 1, and 3 weeks of growth in liquid fermentation. Scale bar = 50 µm.

**Table 3.** Carbon (C) and oxygen (O) composition (%) of IrBPE and UnBPE films degraded by *P. ostreatus* in liquid fermentation.

Sample	Fermentation time (weeks)					
	0		1		3	
	C	O	C	O	C	O
<b>IrBPE</b>	74.48 <sup>a</sup> ± 0.27	7.37 <sup>b</sup> ± 1.22	74.92 <sup>a</sup> ± 0.84	7.39 <sup>b</sup> ± 1.83	49.35 <sup>b</sup> ± 1.90	12.27 <sup>a</sup> ± 1.83
<b>UnBPE</b>	74.71 <sup>a</sup> ± 1.05	6.98 <sup>a</sup> ± 0.96	74.32 <sup>a</sup> ± 2.01	7.96 <sup>a</sup> ± 0.74	74.53 <sup>a</sup> ± 1.73	7.36 <sup>a</sup> ± 1.09

The mean and standard deviation ( $\pm$ ) of triplicate experiments is reported. Measurements within the same row with different letters are significantly different. The statistical significance level for the ANOVA is  $p < 0.05$  according to the Tukey test (see Sect. 2.7).

Table 3 shows the carbon and oxygen composition of the surface of the IrBPE and UnBPE films. EDX analysis was used in combination with SEM to quantify the changes in the percentage of elemental composition of BPE films. The most abundant elements on the surface of both films after biodegradation were carbon (C) and oxygen (O). The analysis demonstrated that the percentage of C on the surface of IrBPE decreased (25.13 %), while the percentage of O significantly increased (4.9 %) after 3 weeks of growth of *P. ostreatus*. For the UnBPE samples, the percentages of C and O remained constant during the fermentation.

#### 4. DISCUSSION

Lac activity increased during the first week and decreased at the second week when MnP production started in all the cultures. The enzymatic activity of Lac, MnP, and LiP declined after week 3, which correlates with the decrease in the growth of *P. ostreatus* in all the cultures. UnP production increased after week 2 and until the end of the fermentation. These results showed that Lac, MnP, UnP, and LiP enzymes acted synergistically. It is suggested that Lac started the degradation of BPE and UnP, LiP, and MnP are involved in the last steps of the biodegradation process due to their large cavities, which would allow a more efficient degradation process (Santacruz Juárez *et al.*, 2021). The maximum Lac activity ( $E_{max}$ ) was observed after 10 d of fermentation, demonstrating that Lac was involved in the initial degradation of BPE, causing the formation of free radicals (Kurt and Buyukalaca, 2010; Da Luz *et al.*, 2013; Bánfi *et al.*, 2015). In addition, the hydroperoxides formed during its UV-B irradiation catalyzed the biodegradation of IrBPE by Lac (Chaurasia *et al.*, 2015). In the present research, MnP production by *P. ostreatus* started at week 2 in all cultures. Eichlerová *et al.* (2000) also found a maximum MnP activity ( $E_{max}$ ) after 14 d of incubation of *P. ostreatus* cultures grown on nitrogen-limited Kirk medium (Tien and Kirk, 1988). Furthermore, González-Márquez *et al.* (2024) studied the enzyme production of *P. ostreatus* grown on recycled PE and commercial PE films treated with UV-B radiation, finding an  $E_{max}$  of LiP activity of 2432 and 2502 U/L, respectively. In the present study, a higher  $E_{max}$  of LiP

(2789 U/L) was observed in cultures supplemented with IrBPE than that  $E_{\max}$  of LiP showed previously.

In the present work, *P. ostreatus* produced UnP from week 3 and until the end of the fermentation. González-Rodríguez *et al.* (2023) also found UnP production by *Agrocybe aegerita* when grown on different dilutions of vinasse in liquid fermentation. However, González-Márquez *et al.* (2024) reported that *P. ostreatus* was able to produce UnP when grown on recycled PE films treated with UV-B radiation, from week 2 and until the end of the fermentation. Our results confirmed that UnP was involved in the final steps of polyethylene biodegradation, acting once Lac and MnP production decrease. It is shown that BPE films exhibited a degree of oxidation before degradation by *P. ostreatus*, which favored the oxidation of the polymer chain by fungal enzymes.

Yagoubi *et al.* (2015) reported that polymer chain oxidation increases after exposure to UV-B radiation, which was confirmed in our research. FTIR spectra of the BPE surface showed an increase in absorbance of the bands between  $1100-800\text{ cm}^{-1}$ ,  $1800-1680\text{ cm}^{-1}$  and  $3600$  to  $3300\text{ cm}^{-1}$ , which correspond to double bonds, carbonyl groups and hydroxyl groups, respectively.

IrBPE showed significant structural changes because exposure to UV-B radiation, which modified the functional groups in the polymer chain as well as the hydrophobic surface.

Martínez-Romo *et al.* (2018) found that the area under the curve between  $1490-1440\text{ cm}^{-1}$  increased in the FTIR spectra of LDPE, HDPE, oxodegradable PE, and biodegradable PE exposed to UV-B irradiation, which shows the cleavage of the polymer chain. In the present study, the area under the curve of the FTIR spectra for IrBPE and UnBPE showed the branching of the polymer chain, which allowed the formation of short polymer chain.

Furthermore, the FTIR spectra of the BPE surface showed an increase in absorbance in the range of  $3600-3300\text{ cm}^{-1}$  (related to OH groups), indicating oxidation of the polymer chain after BPE degradation, which agrees with previous results (Martínez *et al.*, 2021). In addition, CI increased in IrBPE due to oxidation caused by UV-B radiation, as previously showed (Martínez *et al.*, 2021). Furthermore, Hakkarainen and Albertsson (2004) reported that vinyl groups promoted the formation of hydroperoxide groups in PE degradation. In the present research, BPE films showed an increase in CI, VI, and HI values at week 2 of fermentation, showing that oxidation reactions occurred during this time due to the production of extracellular enzymes (*i.e.* Lac, MnP, LiP). Martínez-Romo *et al.* (2015) reported that a decreased in the CI, VI, and HI values, showing the metabolization of PE, as observed in IrBPE samples after week 2 fungal growth.

Adithama *et al.* (2023) reported that the decrease in hydrophobicity of BPE films was due to the formation of biofilm on their surface, which altered the physicochemical properties of the BPE, changing the concentration of functional groups and surface morphology. Several studies have been carried out on biodegradation of LDPE pretreated with radiation, in which a significant decrease in the surface hydrophobicity of the samples was observed (Da Luz *et al.*, 2013; Gómez-Méndez *et al.*, 2018; González-Márquez *et al.*, 2024). In the present work, IrBPE films also showed a significant decrease in surface hydrophobicity.

IrBPE showed a fragmented surface as a result of the synergistic effect of photobiodegradation. It has been reported that *P. ostreatus* is an option for PE biodegradation due to its enzyme production, which is involved in the formation of oxidizing groups that modify the hydrophobic nature of the polymer surface (Da Luz *et al.*, 2013; Gómez-Méndez *et al.*, 2018; Jaiswal *et al.*, 2022; Gowthami *et al.*, 2023; Ratuchne *et al.*, 2023).

EDX analysis of the elemental composition of BPE films after degradation by *P. ostreatus* provided evidence of oxidation solely of the IrBPE polymer chain, with an increase in the oxygen percentage. Additionally, the decrease in carbon percentage after week 3 of liquid fermentation indicated the loss of molecular weight of the polymer film, which was related to the onset of UnP enzyme production by *P. ostreatus*.

## 5. CONCLUSION

*P. ostreatus* was capable to degrade BPE films. The chemical and morphological structure of the BPE was modified after 20 d of fungal growth, which was demonstrated by the increase of the surface hydrophilicity, and the carbonyl, vinyl, and hydroxyl indices. IrBPE showed fractures on the surface, as well as a decrease in carbon content, and an increase in oxygen content. These results show that low-density polyethylene commercially labeled as biodegradable enhanced its biodegradation when exposed to pretreatment with UV-B radiation. *P. ostreatus* is a promising organism to be used in the BPE degradation for its enzymatic production capabilities.

## ACKNOWLEDGMENTS

We thank the National Council of Humanities, Sciences, and Technologies (CONAHCyT) for providing a MSc. scholarship to Ariadna Denisse Andrade-Alvarado (No. CVU 1170027).

## AUTHOR CONTRIBUTION

Ariadna Denisse Andrade-Alvarado performed the experimental work, analyzed data, and wrote the first draft of the manuscript. Angel González-Márquez performed the experimental work. Rosario González-Mota and Carmen Sánchez planned the experiments, conceived the initial idea, supervised the research, and analyzed data. Carmen Sánchez wrote the final version of the manuscript. All authors read and approved the final version of the manuscript.

## CONFLICT OF INTERESTS

The authors declare that there is no conflict of interest.

## REFERENCES

- Adithama, R.M., Munifah, I., Yanto, D.H.Y., Meryandini, A. 2023. Biodegradation of low-density polyethylene microplastic by new halotolerant bacteria isolated from saline mud in Bledug Kuwu, Indonesia. *Bioresource Technol. Rep.* 22, 101466. <https://doi.org/10.1016/j.biteb.2023.101466>
- Albertsson, A.C., Andersson, S.O., Karlsson, S. 1987. The mechanism of biodegradation of polyethylene. *Polym. Degrad. Stab.* 18(1), 73–87. [https://doi.org/10.1016/0141-3910\(87\)90084-X](https://doi.org/10.1016/0141-3910(87)90084-X)
- Ali, S.S., Elsamahy, T., Al-Tohamy, R., Zhu, D., Mahmoud, Y.A.-G., Koutra, E., Metwally, M.A., Kornaros, M., Sun, J. 2021. Plastic wastes biodegradation: Mechanisms, challenges,

and future prospects. *Sci. Total Environ.* 780, 146590. <https://doi.org/10.1016/j.scitotenv.2021.146590>

Amobonye, A., Bhagwat, P., Singh, S., Pillai, S. 2021. Plastic biodegradation: Frontline microbes and their enzymes. *Sci. Total Environ.* 759, 143536. <https://doi.org/10.1016/j.scitotenv.2020.143536>

Arora, D.S., Gill, P.K. 2001. Comparison of two assay procedures for lignin peroxidase. *Enzyme Microb. Technol.* 28(7–8), 602–605. [https://doi.org/10.1016/S0141-0229\(01\)00302-7](https://doi.org/10.1016/S0141-0229(01)00302-7)

Bánfi, R., Pohner, Z., Kovács, J., Luzics, S., Nagy, A., Dudás, M., Tanos, P., Márialigeti, K., Vajna, B. 2015. Characterisation of the large-scale production process of oyster mushroom (*Pleurotus ostreatus*) with the analysis of succession and spatial heterogeneity of lignocellulolytic enzyme activities. *Fungal Biol.* 119(12), 1354–1363. <https://doi.org/10.1016/j.funbio.2015.10.003>

Bertolacci, L., Goldoni, L., Zych, A., Athanassiou, A. 2022. Biocatalytic oxidation of polyethylene by *Agrocybe aegerita* mycelium. *Polym. Degrad. Stab.* 199, 109911. <https://doi.org/10.1016/j.polymdegradstab.2022.109911>

Bettin, F., da Rosa, L.O., Montanari, Q., Calloni, R., Gaio, T.A., Malvessi, E., da Silveira, M.M., Dillon, A.J.P. 2011. Growth kinetics, production, and characterization of extracellular laccases from *Pleurotus sajor-caju* PS-2001. *Process Biochem.* 46(3), 758–764. <https://doi.org/10.1016/j.procbio.2010.12.002>

Burelo, M., Hernández-Varela, J.D., Medina, D.I., Treviño-Quintanilla, C.D. 2023. Recent developments in bio-based polyethylene: Degradation studies, waste management and recycling. *Heliyon* 9(11), e21374. <https://doi.org/10.1016/j.heliyon.2023.e21374>

Camacho-Morales, R.L., Gerardo-Gerardo, J.L., Guillén-Navarro, K., Sánchez, J.E. 2017. Producción de enzimas ligninolíticas durante la degradación del herbicida paraquat por hongos de la pudrición blanca. *Rev. Argent. Microbiol.* 49(2), 189–196. <https://doi.org/10.1016/j.ram.2016.11.004>

Chamas, A., Moon, H., Zheng, J., Qiu, Y., Tabassum, T., Jang, J.H., Abu-Omar, M., Scott, S.L., Suh, S. 2020. Degradation rates of plastics in the environment. *ACS Sustainable Chem. Eng.* 8(9), 3494–3511. <https://doi.org/10.1021/acssuschemeng.9b06635>

Chaurasia, K.P., Bharati, L.S., Sharma, M., Singh, S.K., Yadav, R.S., Yadava, S. 2015. Fungal laccases and their biotechnological significances in the current perspective: A review. *Curr. Org. Chem.* 19(19), 1916–1934. <https://doi.org/10.2174/1385272819666150629175237>

Da Luz, J.M.R., Paes, S.A., Nunes, M.D., da Silva, M. de C.S., Kasuya, M.C.M. 2013. Degradation of oxo-biodegradable plastic by *Pleurotus ostreatus*. PLoS One 8(8), e69386. <https://doi.org/10.1371/journal.pone.0069386>

Dimassi, S.N., Hahladakis, J.N., Chamkha, M., Ahmad, M.I., Al-Ghouti, M.A., Sayadi, S. 2024. Investigation on the effect of several parameters involved in the biodegradation of polyethylene (PE) and low-density polyethylene (LDPE) under various seawater environments. Sci. Total Environ. 912, 168870. <https://doi.org/10.1016/j.scitotenv.2023.168870>

Eichlerová, I., Homolka, L., Nerud, F., Zadrazil, F., Baldrian, P., Gabriel, J. 2000. Screening of *Pleurotus ostreatus* isolates for their ligninolytic properties during cultivation on natural substrates. Biodegradation 11(5), 279–287. <https://doi.org/10.1023/A:1011165919887>

Eriksen, M.K., Christiansen, J.D., Daugaard, A.E., Astrup, T.F. 2019. Closing the loop for PET, PE, and PP waste from households: Influence of material properties and product design for plastic recycling. Waste Manag. 96, 75–85. <https://doi.org/10.1016/j.wasman.2019.07.005>

Flury, M., Narayan, R. 2021. Biodegradable plastic as an integral part of the solution to plastic waste pollution of the environment. Curr. Opin. Green Sustainable Chem. 30, 100490. <https://doi.org/10.1016/j.cogsc.2021.100490>

Fotopoulou, K.N., Karapanagioti, H.K. 2017. Degradation of various plastics in the environment. In: Takada, H., Karapanagioti, H.K. (Ed), Hazardous Chemicals Associated with Plastics in the Marine Environment: The Handbook of Environmental Chemistry, Springer. Cham. pp. 71-92.

Ghosh, K., Jones, B.H. 2021. Roadmap to biodegradable plastics—Current state and research needs. ACS Sustainable Chem. Eng. 9(18), 6170–6187. <https://doi.org/10.1021/acssuschemeng.1c00801>

Gómez-Méndez, L.D., Moreno-Bayona, D.A., Poutou-Piñales, R.A., Salcedo-Reyes, J.C., Pedroza-Rodríguez, A.M., Vargas, A., Bogoya, J.M. 2018. Biodeterioration of plasma pretreated LDPE sheets by *Pleurotus ostreatus*. PLoS One 13(9), e0203786. <https://doi.org/10.1371/journal.pone.0203786>

González-Márquez, A., Andrade-Alvarado, A.D., González-Mota, R., Sánchez, C. 2024. Enhanced degradation of phototreated recycled and unused low-density polyethylene films by *Pleurotus ostreatus*. World J. Microbiol. Biotechnol. 40(10), 309. <https://doi.org/10.1007/s11274-024-04116-6>

González-Márquez, A. and Sánchez, C. 2024. Mycelial growth and production of laccase and peroxidases by *Pleurotus ostreatus* and *Agrocybe aegerita* in liquid fermentation. Mex. J. Biotechnol. 9(3), 36-49. <https://doi.org/10.29267/mxjb.2024.9.3.36>



González-Rodríguez, S., Trueba-Santiso, A., Lu-Chau, T.A., Moreira, M.T., Eibes, G. 2023. Valorization of bioethanol by-products to produce unspecific peroxygenase with *Agrocybe aegerita*: Technological and proteomic perspectives. *New Biotechnol.* 76, 63–71. <https://doi.org/10.1016/j.nbt.2023.05.001>

Gowthami, A., Syed Marjuk, M., Raju, P., Nanthini Devi, K., Santhanam, P., Dinesh Kumar, S., Perumal, P. 2023. Biodegradation efficacy of selected marine microalgae against Low-Density Polyethylene (LDPE): An environment friendly green approach. *Mar. Pollut. Bull.* 190, 114889. <https://doi.org/10.1016/j.marpolbul.2023.114889>

Hakkarainen, M., Albertsson, AC. 2024. Environmental Degradation of Polyethylene. In: Albertsson, AC. (Ed), *Long Term Properties of Polyolefins: Advances in Polymer Science*, Springer. Berlin. pp. 177-200.

Han, Y., Wang, R., Wang, D., Luan, Y. 2024. Enzymatic degradation of synthetic plastics by hydrolases/oxidoreductases. *Int. Biodeterior. Biodegrad.* 189, 105746. <https://doi.org/10.1016/j.ibiod.2024.105746>

He, Y., Deng, X., Jiang, L., Hao, L., Shi, Y., Lyu, M., Zhang, L., Wang, S. 2024. Current advances, challenges, and strategies for enhancing the biodegradation of plastic waste. *Sci. Total Environ.* 906, 167850. <https://doi.org/10.1016/j.scitotenv.2023.167850>

Jaiswal, P.B., Pushkar, B.K., Maikap, K., Mahanwar, P.A. 2022. Abiotic aging assisted bio-oxidation and degradation of LLDPE/LDPE packaging polyethylene film by stimulated enrichment culture. *Polym. Degrad. Stab.* 206, 110156. <https://doi.org/10.1016/j.polymdegradstab.2022.110156>

Kaing, V., Guo, Z., Sok, T., Kodikara, D., Breider, F., Yoshimura, C. 2024. Photodegradation of biodegradable plastics in aquatic environments: Current understanding and challenges. *Sci. Total Environ.* 911, 168539. <https://doi.org/10.1016/j.scitotenv.2023.168539>

Kumar, A., Chandra, R. 2020. Ligninolytic enzymes and its mechanisms for degradation of lignocellulosic waste in environment. *Heliyon.* 6(2), e03170. <https://doi.org/10.1016/j.heliyon.2020.e03170>

Kurt, S., Buyukalaca, S. 2010. Yield performances and changes in enzyme activities of *Pleurotus spp.* (*P. ostreatus* and *P. sajor-caju*) cultivated on different agricultural wastes. *Bioresour. Technol.* 101(9), 3164–3169. <https://doi.org/10.1016/j.biortech.2009.12.011>

Kyaw, B.M., Champakalakshmi, R., Sakharkar, M.K., Lim, C.S., Sakharkar, K.R. 2012. Biodegradation of Low Density Polythene (LDPE) by *Pseudomonas* Species. *Indian J. Microbiol.* 52(3), 411–419. <https://doi.org/10.1007/s12088-012-0250-6>

Lamour, G., Hamraoui, A., Buvailo, A., Xing, Y., Keuleyan, S., Prakash, V., Eftekhari-Bafrooei, A., Borguet, E. 2010. Contact angle measurements using a simplified experimental setup. *J. Chem. Educ.* 87(12), 1403–1407. <https://doi.org/10.1021/ed100468u>

Lear, G., Kingsbury, J.M., Franchini, S., Gambarini, V., Maday, S.D.M., Wallbank, J.A., Weaver, L., Pantos, O. 2021. Plastics and the microbiome: impacts and solutions. *Environ. Microbiome*. 16(1), 2. <https://doi.org/10.1186/s40793-020-00371-w>

Martínez, K.I., González-Mota, R., Soto-Bernal, J.J., Rosales-Candelas, I. 2021. Evaluation by IR spectroscopy of the degradation of different types of commercial polyethylene exposed to UV radiation and domestic compost in ambient conditions. *J. Appl. Polym. Sci.* 138(14). <https://doi.org/10.1002/app.50158>

Martínez-Romo, A., González-Mota, R., Soto-Bernal, J.J., Rosales-Candelas, I. 2015. Investigating the degradability of HDPE, LDPE, PE-BIO, and PE-OXO Films under UV-B Radiation. *J. Spectrosc.* 2015, 1–6. <https://doi.org/10.1155/2015/586514>

Martínez-Romo, A., González-Mota, R., Soto-Bernal, J.J., Rosales-Candelas, I. 2018. LDPE Oxidation by CO<sub>2</sub> Laser Radiation (10.6 μm). *Int. J. Polym. Sci.* 2018, 1–5. <https://doi.org/10.1155/2018/5150673>

Moshood, T., Nawanir, G., Mahmud, F., Mohamad, F., Ahmad, M., Abdul Ghani, A. 2021. Expanding policy for biodegradable plastic products and market dynamics of bio-based plastics: Challenges and opportunities. *Sustainability*. 13(11), 6170. <https://doi.org/10.3390/su13116170>

Ocaña-Romo, E., Rodríguez-Nava C.O., Sánchez, C. 2024. Oxidases production by *Trametes versicolor* grown on green waste and on polyurethane foam in solid-state fermentation: A comparative study. *Mex. J. Biotechnol.* 9(2), 51-64. <https://doi.org/10.29267/mxjb.2024.9.2.51>

Okal, E.J., Heng, G., Magige, E.A., Khan, S., Wu, S., Ge, Z., Zhang, T., Mortimer, P.E., Xu, J. 2023. Insights into the mechanisms involved in the fungal degradation of plastics. *Ecotoxicol. Environ. Saf.* 262, 115202. <https://doi.org/10.1016/j.ecoenv.2023.115202>

Okoffo, E.D., Donner, E., McGrath, S.P., Tscharke, B.J., O'Brien, J.W., O'Brien, S., Ribeiro, F., Burrows, S.D., Toapanta, T., Rauert, C., Samanipour, S., Mueller, J.F., Thomas, K.V. 2021. Plastics in biosolids from 1950 to 2016: A function of global plastic production and consumption. *Water Res.* 201, 117367. <https://doi.org/10.1016/j.watres.2021.117367>

Patel, D., Mamtora, D., Kamath, A., Shukla, A. 2022. Rogue one: A plastic story. *Mar. Pollut. Bull.* 177. <https://doi.org/10.1016/j.marpolbul.2022.113509>

Prata, J.C., Reis, V., Paço, A., Martins, P., Cruz, A., da Costa, J.P., Duarte, A.C., Rocha-Santos, T. 2020. Effects of spatial and seasonal factors on the characteristics and carbonyl index of (micro)plastics in a sandy beach in Aveiro, Portugal. *Sci. Total Environ.* 709, 135892. <https://doi.org/10.1016/j.scitotenv.2019.135892>

Ratuchne, A., Lonardoní, E.A., Bueno, C.E., Reis, G.F., Rezende, M.I., Urbano, A., Biz, G., de Almeida, R.S.C., Panagio, L.A. 2023. *Pleurotus ostreatus* and a novel fungal composite:

Development and bioremediation of plastic wastes. Res. Conserv. Recycl. Adv. 19, 200167. <https://doi.org/10.1016/j.rcradv.2023.200167>

Restrepo-Flórez, J.-M., Bassi, A., Thompson, M.R. 2014. Microbial degradation and deterioration of polyethylene – A review. Int. Biodeterior. Biodegrad. 88, 83–90. <https://doi.org/10.1016/j.ibiod.2013.12.014>

Ríos-González, N.S., González-Márquez, Á., Sánchez, C. 2019. Growth and esterase activity of *Fusarium culmorum* grown in di (2-ethyl hexyl) phthalate in liquid fermentation. Mex. J. Biotechnol. 4(1), 51–60. <https://doi.org/10.29267/mxjb.2019.4.1.51>

Sánchez, C. 2020. Fungal potential for the degradation of petroleum-based polymers: An overview of macro- and microplastics biodegradation. Biotechnol. Adv. 40, 107501. <https://doi.org/10.1016/j.biotechadv.2019.107501>

Sánchez, C. 2021. Microbial capability for the degradation of chemical additives presents in petroleum-based plastic products: A review on current status and perspectives. J. Hazard. Mater. 402, 123534. <https://doi.org/10.1016/j.jhazmat.2020.123534>

Skariyachan, S., Taskeen, N., Kishore, A.P., Krishna, B.V. 2022. Recent advances in plastic degradation – From microbial consortia-based methods to data sciences and computational biology driven approaches. J. Hazard. Mater. 426, 128086. <https://doi.org/10.1016/j.jhazmat.2021.128086>

Spina, F., Tummino, M.L., Poli, A., Prigione, V., Ilieva, V., Cocconcelli, P., Puglisi, E., Bracco, P., Zanetti, M., Varese, G.C. 2021. Low density polyethylene degradation by filamentous fungi. Environ. Pollut. 274, 116548. <https://doi.org/10.1016/j.envpol.2021.116548>

Taghavi, N., Udugama, I.A., Zhuang, W.-Q., Baroutian, S. 2021. Challenges in biodegradation of non-degradable thermoplastic waste: From environmental impact to operational readiness. Biotechnol. Adv. 49, 107731. <https://doi.org/10.1016/j.biotechadv.2021.107731>

Tiago, G.A.O., Mariquito, A., Martins-Dias, S., Marques, A.C. 2023. The problem of polyethylene waste – recent attempts for its mitigation. Sci. Total Environ. 892, 164629. <https://doi.org/10.1016/j.scitotenv.2023.164629>

Tien, M. and Kirk, T. 1988. Lignin peroxidase of *Phanerochaete chrysosporium*. Met. Enzymol. 161, 238-249. [https://doi.org/10.1016/0076-6879\(88\)61025-1](https://doi.org/10.1016/0076-6879(88)61025-1).

Volke-Sepúlveda, T., Saucedo-Castañeda, G., Gutiérrez-Rojas, M., Manzur, A., Favela-Torres, E. 2002. Thermally treated low density polyethylene biodegradation by *Penicillium pinophilum* and *Aspergillus niger*. J. Appl. Polym. Sci. 83(2), 305–314. <https://doi.org/10.1002/app.2245>

- Yagoubi, W., Abdelhafidi, A., Sebaa, M., Chabira, S.F. 2015. Identification of carbonyl species of weathered LDPE films by curve fitting and derivative analysis of IR spectra. *Polym. Testing*. 44, 37–48. <https://doi.org/10.1016/j.polymertesting.2015.03.008>
- Yuan, X., Kumar, N.M., Brigljević, B., Li, S., Deng, S., Byun, M., Lee, B., Lin, C.S.K., Tsang, D.C.W., Lee, K.B., Chopra, S.S., Lim, H., Ok, Y.S. 2022. Sustainability-inspired upcycling of waste polyethylene terephthalate plastic into porous carbon for CO<sub>2</sub> capture. *Green Chem.* 24(4), 1494–1504. <https://doi.org/10.1039/d1gc03600a>
- Zhang, H., Huang, Y., Shen, J., Xu, F., Hou, H., Xie, C., Wang, B., An, S. 2024. Mechanism of polyethylene and biodegradable microplastic aging effects on soil organic carbon fractions in different land-use types. *Sci. Total Environ.* 912, 168961. <https://doi.org/10.1016/j.scitotenv.2023.168961>
- Zhang, J., Gao, D., Li, Q., Zhao, Y., Li, L., Lin, H., Bi, Q., Zhao, Y. 2020. Biodegradation of polyethylene microplastic particles by the fungus *Aspergillus flavus* from the guts of wax moth *Galleria mellonella*. *Sci. Total Environ.* 704, 135931. <https://doi.org/10.1016/j.scitotenv.2019.135931>
- Zhang, Y., Pedersen, J.N., Eser, B.E., Guo, Z. 2022. Biodegradation of polyethylene and polystyrene: From microbial deterioration to enzyme discovery. *Biotechnol. Adv.* 60, 107991. <https://doi.org/10.1016/j.biotechadv.2022.107991>
- Zhou, J., Jia, R., Brown, R.W., Yang, Y., Zeng, Z., Jones, D.L., Zang, H. 2023. The long-term uncertainty of biodegradable mulch film residues and associated microplastics pollution on plant-soil health. *J. Hazard. Mater.* 442, 130055. <https://doi.org/10.1016/j.jhazmat.2022.130055>